High-Order Flux Reconstruction Schemes for LES on Tetrahedral Meshes

Jonathan R. Bull and Antony Jameson

Abstract The use of the high-order Flux Reconstruction (FR) spatial discretization scheme for LES on unstructured meshes is investigated. Simulations of the compressible Taylor-Green vortex at $Re = 1600$ demonstrate that the FR scheme has low numerical dissipation and accurately reproduces the turbulent energy cascade at low resolution, making it ideal for high-order LES. To permit the use of subgrid-scale models incorporating explicit filtering on tetrahedral meshes, a high-order filter acting on the modal form of the solution (i.e. the Dubiner basis functions) is developed. The WALE-Similarity mixed (WSM) model using this filter is employed for LES of the flow over a square cylinder at $Re = 21,400$, obtaining reasonable agreement with experiments. Future research will be directed at improved SGS models and filters and at developing high-order hybrid RANS/LES methods.

1 Introduction

Advances in computing hardware are bringing large eddy simulation (LES) of real applications at high Reynolds numbers into the realms of possibility. However, most LES solvers are based on dissipative second-order accurate ($p = 2$) numerical schemes which have poor wave propagation properties. This limits the usefulness of LES in many applications where the turbulent motions must be accurately resolved far downstream from their source. These severe problems can be overcome by using high-order accurate ($p > 2$) spatial discretizations such as Discontinuous Galerkin (DG) [17], Spectral Difference (SD) [23] and Flux Reconstruction (FR) [18] methods. A family of energy-stable FR schemes have been developed by the Aerospace Computing Lab (ACL) at Stanford University [34] based on the work of Huynh [18]. By varying a stabilization parameter, a range of existing schemes can be recovered including nodal DG and SD. The FR method has several advantages over DG: it

Dept of Aeronautics and Astronautics, Stanford University, CA 94305, USA, e-mail: jbull@stanford.edu

is conceptually simpler, easier to implement (including on unstructured meshes) and cheaper to compute due to casting the equations in differential form (avoiding costly integration procedures). The FR schemes are proposed as an ideal basis for turbulence-resolving simulations due to their flexibility, stability and low numerical dissipation. As a demonstration of this, the compressible Taylor-Green vortex benchmark problem at $Re = 1600$ was simulated. Results show that the FR schemes are highly accurate compared to DNS and stable at low resolution.

Various stabilized high-order schemes have been successfully used for implicit LES (ILES) of turbulent flows (i.e. exploiting numerical dissipation as an ersatz turbulence model) [6, 5, 21]. Turbulent simulations using the FR method to recover the SD scheme have also been successful, including channel flow at $Re_\tau = 400$ [22] and transitional flow over an airfoil at $Re = 60\,000$ [9]. However, in the case of separating flow over a square cylinder at $Re = 21\,400$ it was found that a subgrid-scale (SGS) model was needed to improve accuracy in the turbulent wake [24]. Other studies have also shown that high-order schemes benefit from the inclusion of an SGS model [30, 13, 11]. To permit the use of advanced SGS models based on explicit filtering, including the similarity and dynamic models, discrete high-order filters were developed for hexahedral elements by Lodato, Castonguay and Jameson as a tensor product of 1D filter operators [24]. The filters were designed to have consistent cutoff length scales at different polynomial orders and at all solution points within the element. Support for the filters is limited to the element interior to maintain the efficient parallelization of the FR method. In this paper, a filter for tetrahedral elements is developed, enabling SGS models based on explicit filtering to be applied to unstructured meshes. The filter acts on the modal form of the solution and is based on the Spectral Vanishing Viscosity (SVV) stabilization technique for DG methods [20, 16, 31, 28]. The flow over a square cylinder at $Re = 21\,400$ was simulated using the FR method with the WALE-Similarity Mixed (WSM) model, with reasonably accurate results obtained on a relatively coarse unstructured mesh. Future research will develop better SGS models and near-wall models including high-order hybrid RANS-LES techniques.

2 High-Order Flux Reconstruction

The compressible Navier-Stokes equations are discretized using the high-order Flux Reconstruction scheme. We write the equations in conservative form in a 3D domain Ω with spatial coordinates $\mathbf{x} = \{x_1, x_2, x_3\}$ and time t:

$$\frac{\partial \mathbf{u}}{\partial t} + \frac{\partial \mathbf{f}}{\partial \mathbf{x}} = 0 \,, \tag{1}$$

where $\mathbf{u} = (\rho \ \rho u \ \rho v \ \rho w \ \rho e)^T$ are the conservative variables and $\mathbf{f}$ is the flux. The domain is split into non-overlapping elements Ω_i. Elements are transformed to a reference element described by local coordinates $\xi = \{\xi_1, \xi_2, \xi_3\}$. For simplicity,

we consider the reference element in one dimension ($\xi = [-1:1]$) and transform the 1D analog of (1) to the reference coordinates. Inside the reference element a degree $p = N-1$ polynomial is defined on a set of N solution points, resulting in an Nth-order accurate scheme. The Gauss-Legendre quadrature points (Figure 1) are chosen as the solution points as they were found to minimize aliasing errors for nonlinear problems [19]. The Gauss-Lobatto points are used as the flux points (Figure 1). The piecewise-continuous pth-order solution polynomial u is defined

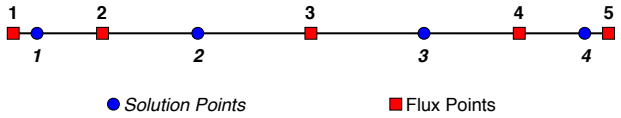

Fig. 1 Location of solution and flux points in 1D

$$u(\xi) = \sum_{i=1}^{N} u_i l_i(\xi) \,, \tag{2}$$

where u_i are the nodal solution values and l_i is a set of basis functions, in this case the Lagrange polynomials. A similar expression is used to obtain the $(p+1)$th-order flux polynomial f. Note that the flux is discontinuous across element boundaries; common interface fluxes are found using a two-point upwind-biased flux formula such as Roe's method [32]. The next step is to construct a globally continuous flux polynomial. In the FR method this is achieved by adding a flux correction polynomial Δf to the discontinuous flux f. The correction satisfies: (a) $f + \Delta f$ equals the common interface fluxes, and (b) the corrected flux optimally represents the discontinuous flux in the element interior. Δf is given by

$$\Delta f(\xi) = [f_L^* - f(-1)]g_L(\xi) + [f_R^* - f(1)]g_R(\xi) \,, \tag{3}$$

where f_L^*, f_R^* are the common interface fluxes at left and right interfaces and $g_L(\xi), g_R(\xi)$ are order $p+2$ polynomial *correction functions* satisfying $g_L(-1) = g_R(1) = 1,\ g_L(1) = g_R(-1) = 0,\ g_L(\xi) = g_R(-\xi)$. Now the corrected, globally C_0-continuous flux f^C is given by $f^C = f + \Delta f$. The final stage of the FR process is to calculate the divergence of f^C at each solution point ξ_i using the expression

$$\frac{\partial f^C}{\partial \xi}(\xi_i) = \sum_{j=1}^{N} f_j \frac{\partial l_j}{\partial \xi}(\xi) + [f_L^* - f(-1)]\frac{\partial g_L}{\partial \xi}(\xi_i) + [f_R^* - f(1)]\frac{\partial g_R}{\partial \xi}(\xi_i). \tag{4}$$

The solution is advanced in time with an explicit Runge-Kutta scheme which avoids the need to construct and invert large matrices. It was shown by Vincent, Castonguay and Jameson [34] that the FR schemes are energy-stable for the linear advection problem if the correction functions g_L and g_R are given by

$$g_L = \frac{(-1)^p}{2}\left[L_p - \left(\frac{\eta_p(c)L_{p-1} + L_{p+1}}{1+\eta_p(c)}\right)\right], \tag{5}$$

$$g_R = \frac{(-1)^p}{2}\left[L_p - \left(\frac{\eta_p(c)L_{p-1} + L_{p+1}}{1+\eta_p(c)}\right)\right], \tag{6}$$

where L_p is the degree p Legendre polynomial, $\eta_p(c) = (c(2p+1)(a_p p!))^2)/2$ and $0 \leq c \leq \infty$ is a user-defined stability parameter. The proof was extended to linear advection-diffusion problems by Castonguay et al. [10]. The baseline case, $c = 0$, corresponds to a nodal DG scheme which is susceptible to aliasing-driven instabilities. The particular choice of $c > 0$ determines the amount of additional stabilizing dissipation and allows one to recover other schemes such as SD [34]. Allaneau and Jameson [3] showed that $c > 0$ corresponds to damping of the highest-order solution mode. Stabilization techniques are commonly used with DG, either by direct filtering [15] or by including an equivalent high-order dissipative term [31, 7]. As a demonstration of the stability and accuracy of FR for turbulent flow computations, results of the compressible Taylor-Green vortex are presented next.

3 Taylor-Green Vortex

The Taylor-Green vortex is a simple yet powerful tool for studying the ability of a numerical method to represent the turbulent energy cascade. Starting from an analytical solution defining a single lengthscale, nonlinear interactions between eddies generate a broadband turbulent spectrum which decays in a well-defined manner. Here, we run the compressible benchmark problem at $Re = 1600$ (part of the 1st and 2nd International Workshops on High-Order CFD Methods [1, 2]) and compare results to high-order DG computations [5] and DNS [12]. Figs. 2 (a)-(d) show the volume-averaged kinetic energy $\langle k \rangle$ and dissipation rate $-d\langle k \rangle/dt$ using FR to recover the fourth-order-accurate SD scheme on regular tetrahedral meshes formed by splitting hexahedral meshes of 16^3, 32^3 and 64^3 elements. On the 64^3 mesh the kinetic energy (Fig. 2 (a)) and dissipation rate (Fig. 2 (b)) predictions match the DNS data [12] and the high-order results at equal resolution [5], showing that numerical dissipation dissipates the turbulent energy at the correct rate. At lower mesh resolution the kinetic energy decays more rapidly, implying that the numerical dissipation is too strong. Fig. 2 (c) shows the results of the third to sixth order accurate SD schemes on the 16^3 tetrahedral mesh. At third order the dissipation peak is shifted to the left, indicating that numerical dissipation is too strong. As the order increases, the accuracy improves, with the biggest change being from third to fourth order. Instabilities tend to occur for orders higher than six, particularly on coarse meshes, implying that fourth order may be optimal for high-order LES. Finally Figure 2 (d) shows an isosurface of the Q criterion at 10.75 seconds, demonstrating the ability of the high-order method to maintain a finely detailed turbulent spectrum after a long time by virtue of the low dissipation.

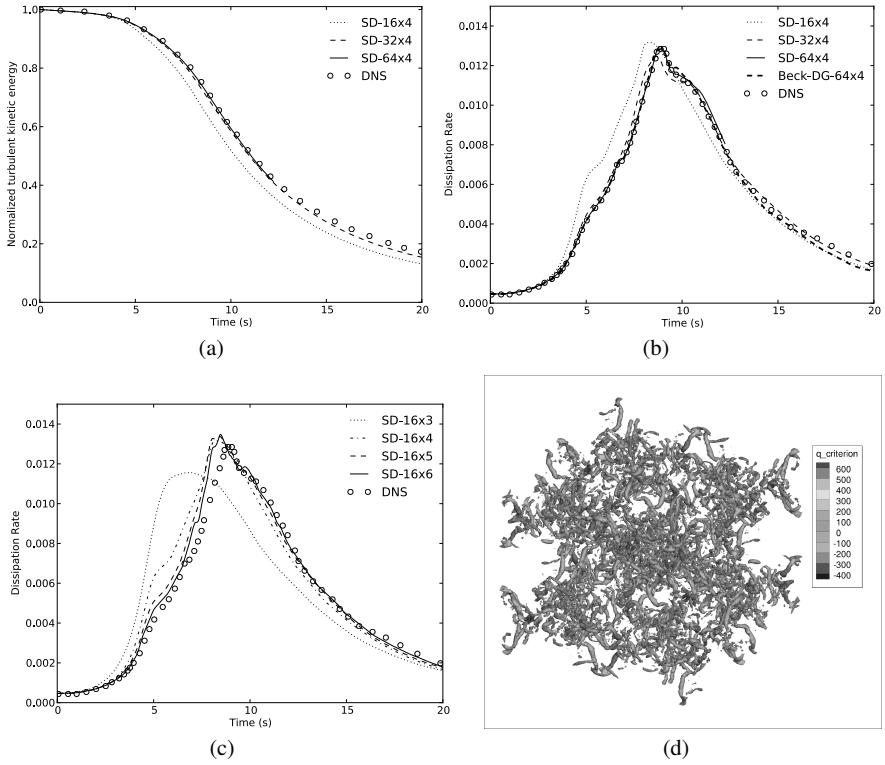

Fig. 2 Taylor-Green vortex results on tetrahedral meshes. (a) Evolution of average kinetic energy $\langle k \rangle$. Dissipation rate $-d\langle k \rangle / dt$ with different (b) meshes and (c) orders. (d) Isosurface of Q-criterion at 10.75 seconds on 64^3 mesh at 4th order, showing vortex filaments. 'SD-$M \times N$' refers to M^3 mesh, Nth-order accurate SD scheme. (**- - -**) 4th-order DG on 64^3 mesh [5]; (○) DNS [12].

4 LES Modeling

Previous work by Lodato, Castonguay and Jameson [24] found that the addition of an SGS model to the SD method improved the accuracy of first and second moments in a separated turbulent flow. A mixed SGS model was employed, comprising the WALE eddy-viscosity model [29] and the similarity model [4]:

$$\tau_{ij} = 2\overline{\rho}[\nu_t \tilde{S}_{ij} - (\overline{\tilde{u}_i \tilde{u}_j} - \overline{\tilde{u}}_i \overline{\tilde{u}}_j)], \tag{7}$$

$$\nu_t = C_w^2 \triangle^2 \frac{(s_{ij}^d s_{ij}^d)^{3/2}}{(S_{ij}^d S_{ij}^d)^{5/2} + (s_{ij}^d s_{ij}^d)^{5/4}}, \tag{8}$$

$$s_{ij}^d = \frac{1}{2}\left[(\partial_j \tilde{u}_i)^2 + (\partial_i \tilde{u}_j)^2\right] - \frac{1}{3}\delta_{ij}(\partial_k \tilde{u}_k)^2, \quad \tilde{S}_{ij} = \frac{1}{2}\left(\frac{\partial \tilde{u}_i}{\partial x_j} + \frac{\partial \tilde{u}_j}{\partial x_i}\right), \tag{9}$$

where $\tilde{(\ldots)}$ denotes a Favre-averaged quantity and $\overline{(\ldots)}$ is an explicitly filtered quantity. The filter width is given by $\triangle = \left[|\det(\mathbf{J}(\xi))|^{1/3}\right]/(p+1)$, where the determinant of the Jacobian $|\det(\mathbf{J})|$ is equivalent to the element volume. It has been found by various authors [37, 36, 35] that mixed formulations overcome the limitations of their component models, providing both sufficient energy draining of the resolved scales and structural representation of the subgrid scales. However, the explicitly filtered terms in the similarity model pose a problem in high-order methods: a high-order filter is required to maintain the overall accuracy of the numerical method. Lodato, Castonguay and Jameson [24] developed a discrete filter by integrating the Gaussian kernel over the quadrature points (dropping the $\tilde{(\ldots)}$ notation for clarity):

$$\overline{u}(\xi_s) = \sum_{i=1}^{N} G(\xi_s - \xi_i) u_i w_i, \tag{10}$$

where u_i are the nodal values of the solution, w_i are the quadrature weights and $G(\xi_s - \xi_i)$ is the Gaussian filter kernel centered at ξ_s evaluated at a point ξ_i. A filter for hexahedral elements is then simply the tensor product of three 1D filters.

An alternative approach in high-order methods is to filter the *modal* form of the solution (in 1D):

$$u = \sum_{i=0}^{p} \hat{u}_i L_i(\xi), \tag{11}$$

where $\hat{u}_i$ are the *modal coefficients* and $L_i(\xi)$ are the normalized Legendre polynomials. Since the Legendre polynomials form an orthogonal basis, the modal form (11) can be viewed as a pseudo-spectrum and the action of damping the high-order modes is analogous to low-pass filtering. Modal filtering is commonly applied as a stabilization technique in high-order methods on structured grids by taking tensor products of 1D modal filters [16, 20, 31]. A natural basis for high-order discretizations on simplex elements (triangles and tetrahedra) is the *Dubiner basis* [14, 33], given by (in 3D):

$$\phi_{ijk}(r,s,t) = P_i^{(0,0)}(a) P_j^{(2i+1,0)}(b) P_k^{(2i+2j+2,0)}(c), \tag{12}$$

$$a = \left(\tfrac{2(1+r)}{-s-t} - 1\right)\left(\tfrac{-s-t}{2}\right),\ b = \left(2\tfrac{1+s}{1-t} - 1\right)\left(\tfrac{1-t}{2}\right),\ c = t\ , \tag{13}$$

where $P_j^{(A,B)}$ is the 1D jth-order Jacobi polynomial and r,s,t are local coordinates on the reference tetrahedron $\mathbf{T}^3 = \{(r,s,t) \in \mathbf{R}^3 | r,s,t \geq -1, r+s+t \leq 0\}$. The Dubiner polynomials (12) form an orthogonal basis $\mathbf{P} = \text{span}\ \{r^i s^j t^k \mid 0 \leq i,j,k \leq p;\ 0 \leq i+j+k \leq p\}$. The tetrahedral modal solution is then expressed as

$$u = \sum_{i+j+k \leq p} \hat{u}_{ijk} \phi_{ijk}(r,s,t). \tag{14}$$

The Dubiner basis can be directly filtered, avoiding the issue of not being able to define a tensor product of 1D operators in simplex elements. Following the work of Meister et al. [28] in 2D, a 3D pth-order exponential filter operator is defined by

$$\overline{u} = \sum_{i+j+k\leq p} \sigma_{ijk}\, \hat{u}_{ijk}\, \phi_{ijk}(r,s,t)\ , \tag{15}$$

$$\sigma_{ijk}(\eta) = \exp(-\alpha\eta^{2p}), \quad \eta = \tfrac{i+j+k}{p+1}, \quad \alpha = C_\sigma p, \tag{16}$$

where C_σ is a filter strength coefficient. It was found that $C_\sigma \approx 0.1$ resulted in good behavior of the similarity model. In future, this parameter could be estimated using a dynamic procedure.

5 LES of Flow over a Square Cylinder

Using the FR method to recover the fourth-order accurate SD scheme, the flow over a square cylinder of side D at $Re = 21,400$ and Mach 0.3 was simulated, for which LDV experimental data is available [27, 26]. The domain measured $21D \times 12D \times 3.2D$ and a tetrahedral mesh of 87,178 elements was generated, which with 20 solution points per element resulted in 1.74M degrees of freedom. A fourth-order five-stage explicit RK scheme was used and a total time of 250 seconds was simulated, with time-averaged quantities calculated over the last 100 seconds (approx. 5 flow-through periods). The WSM model (7) based on the tetrahedral modal filter (15) was used, with the three-layer wall model [8] used within 0.2D of the wall. The computation took around 60 hours on 7 GPUs in the lab's own cluster. Figures 3 (a, b) show the normalized mean streamwise and vertical velocity components $\langle u\rangle/u_B$ and $\langle v\rangle/u_B$ respectively along several vertical lines in the wake. Figures 4 (a, b) show the normalized mean Reynolds stress components $\langle u'u'\rangle/u_B^2$ and $\langle u'v'\rangle/u_B^2$. The high-order LES results on a hexahedral mesh by Lodato and Jameson [24] are also plotted for comparison. Mean velocities are reasonably approximated, but near the cylinder the accuracy deteriorates. The Reynolds stresses are less well predicted, particularly near the cylinder. One reason for the inaccurate results is that the near-wall mesh is quite coarse. Another reason is that the three-layer wall model [8] is not well suited to separated flows, as seen in the first subplot of Figure 3 (a) which shows the mean streamwise velocity profile through the boundary layer on top of the cylinder ($x = 0.0$) compared to LES by Lubcke et al. [25]. It is clear that the recirculation bubble is not predicted by the wall model. The use of more suitable wall modeling approaches is left as a matter for future research.

6 Conclusions

The high-order Flux Reconstruction (FR) method was applied to turbulent flows on tetrahedral meshes. Simulated energy dissipation rates for the Taylor-Green vortex were in excellent agreement with DNS, suggesting that the FR method's low numerical dissipation and good stability make it a strong candidate for high-order LES. A high-order modal filter was developed, enabling the use of SGS models based on explicit filtering including the mixed WALE-similarity model tested here. Results

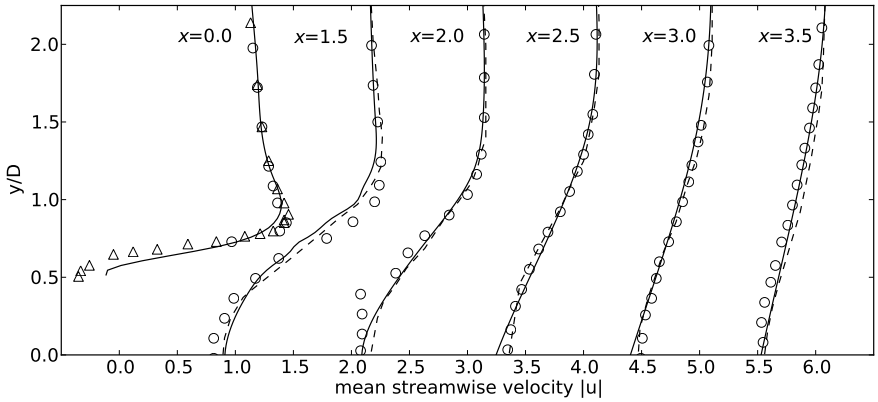

(a) Mean streamwise velocity $\langle u \rangle / u_B$

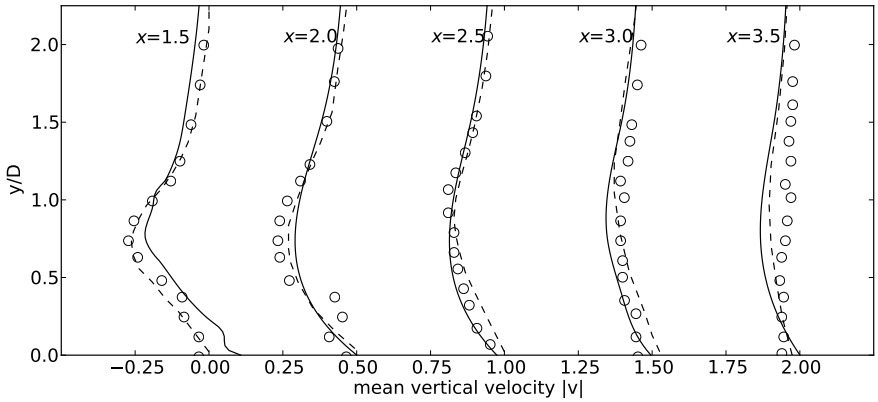

(b) Mean vertical velocity $\langle v \rangle / u_B$

Fig. 3 (a) Mean streamwise and vertical velocity along vertical lines in the wake. (—) current results, (- - -) 4th order SD+WSM on hexahedral mesh by Lodato and Jameson [24], (△) LES by Lubcke et al. [25], (○) LDV experiments by Lyn et al. [27, 26].

of the flow over a square cylinder were reasonably close to experimental data at low mesh resolution. More work is needed to improve the accuracy of high-order LES with the FR method, including studying the sensitivity to the mesh, choice of high-order scheme, order of accuracy, SGS model and wall model. In future, work will focus on modeling of the near-wall region in complex turbulent flows, in particular with hybrid RANS-LES methods. In addition, a high-order dynamic LES method will be developed based on the modal filter. The presented research is a step towards the goal of simulating real-world applications at greater accuracy and lower computational cost than current second-order methods.

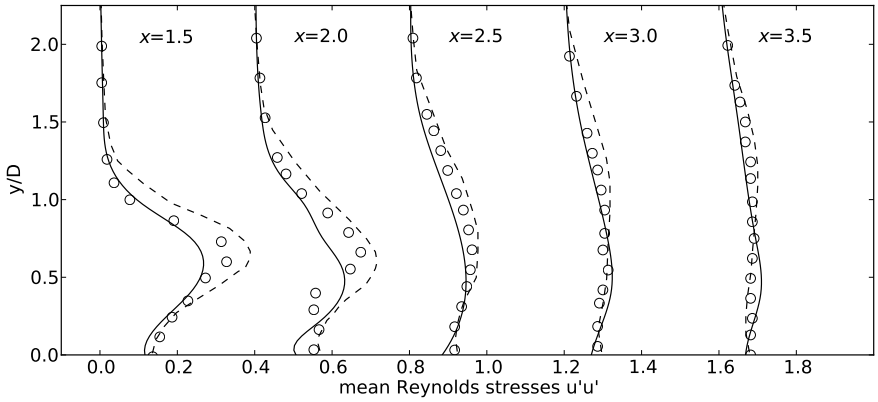

(a) Mean Reynolds stress $\langle u'u' \rangle / u_B^2$

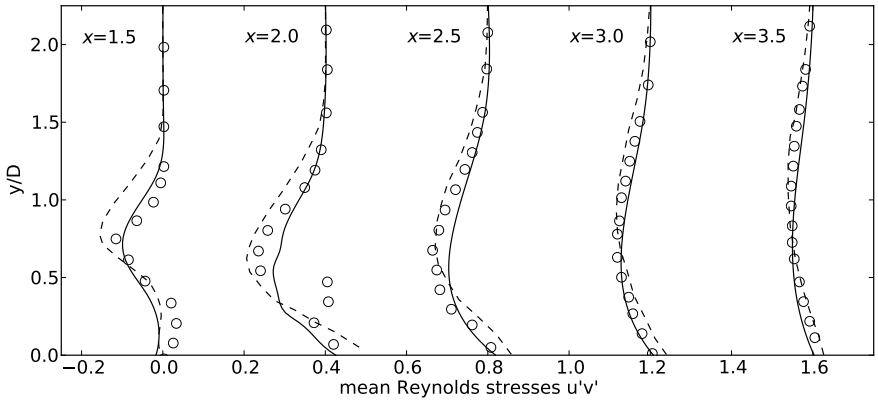

(b) Mean Reynolds stress $\langle u'v' \rangle / u_B^2$

Fig. 4 (a) Mean Reynolds stresses along vertical lines in the wake. (—) current results, (- - -) 4th order SD+WSM on hexahedral mesh by Lodato and Jameson [24], (○) LDV experiments by Lyn et al. [27, 26].

7 Acknowledgments

This research was made possible by the support of the NSF under grant number 1114816, monitored by Dr Leland Jameson, and the Air Force Office of Scientific Research under grant number FA9550-10-1-0418, monitored by Dr Fariba Fahroo.

References

1. 1st international workshop on high-order CFD methods. At the 50th AIAA Aerospace Sciences Meeting, January 7-8 2012, Nashville, Tennessee (2012)
2. 2nd international workshop on high-order CFD methods. At DLR, May 27-28, Cologne, Germany (2013)
3. Allaneau, Y., Jameson, A.: Connections between the filtered discontinous galerkin method and the flux reconstruction approach to high order discretizations. Computer Methods in Applied Mechanics and Engineering pp. 3628–3636 (2011)
4. Bardina, J., Ferziger, J., Reynolds, W.: Improved subgrid-scale models for large-eddy simulation. In: 13th AIAA Fluid and Plasma Dynamics Conference. Snowmass, Colo., July 14-16, 1980 (1980)
5. Beck, A., Gassner, G.: On the accuracy of high-order discretizations for underresolved turbulence simulations. Theoretical and Computational Fluid Dynamics **27**(3-4), 221–237 (2012)
6. Bouffanais, R., Deville, M., Fischer, P., Leriche, E., Weill, D.: Large-eddy simulation of the lid-driven cubic cavity flow by the spectral element method. Journal of Scientific Computing **27**(1-3), 151–162 (2006)
7. Boyd, J.: The legendre–burgers equation: When artificial dissipation fails. Applied Mathematics and Computation **217**, 1949–1964 (2010)
8. Breuer, M., Rodi, W.: Large-eddy simulation of turbulent flow through a straight square duct and a 180 bend. In: Direct and Large-Eddy Simulation I, pp. 273–285. Springer (1994)
9. Castonguay, P., Liang, C., Jameson, A.: Simulation of Transitional Flow over Airfoils using the Spectral Difference Method. AIAA P. **2010-4626** (2010)
10. Castonguay, P., Williams, D., Vincent, P.E., Jameson, A.: Energy stable flux reconstruction schemes for advection–diffusion problems. Comput. Methods Appl. Mech. Engrg. **267**, 400–417 (2013)
11. Chapelier, J.B., Plata, M., Renac, F.: Inviscid and viscous simulations of the Taylor-Green vortex flow using a modal Discontinuous Galerkin approach. AIAA paper 2012-3073 (2012)
12. Debonis, J.: Solutions of the Taylor-Green vortex problem using high-resolution explicit finite difference methods. AIAA Paper 2013-0382 (2013)
13. Diosady, L., Murman, S.: Design of a variational multiscale method for turbulent compressible flows. AIAA paper 2013-2870 (2013)
14. Dubiner, M.: Spectral methods on triangles and other domains. Journal of Scientific Computing **6**(4), 345–390 (1991)
15. Fischer, P., Mullen, J.: Filter-based stabilization of spectral element methods. Comptes Rendus de l'Académie des Sciences-Series I-Mathematics **332**(3), 265–270 (2001)
16. Gottlieb, D., Hesthaven, J.: Spectral methods for hyperbolic problems. Journal of Computational and Applied Mathematics **128**, 83–131 (2001)
17. Hesthaven, J., Warburton, T.: Nodal Discontinuous Galerkin methods: Algorithms, Analysis, and Applications. Springer Verlag (2007)
18. Huynh, H.: A flux reconstruction approach to high-order schemes including discontinuous Galerkin methods. AIAA P. (2007). 18th AIAA Computational Fluid Dynamics Conference, Miami, FL, Jun 25–28
19. Jameson, A., Vincent, P.E., Castonguay, P.: On the non-linear stability of flux reconstruction schemes. Journal of Scientific Computing (2011)
20. Karamanos, G., Karniadakis, G.: A spectral vanishing viscosity method for large-eddy simulations. J. Comput. Phys. **163**(1), 22–50 (2000)
21. Lee, E., Gunzburger, M.: A finite element, filtered eddy-viscosity method for the Navier–Stokes equations with large Reynolds number. J. Math. Anal. Appl. **385**, 384–398 (2012)
22. Liang, C., Premasuthan, S., Jameson, A., Wang, Z.: Large eddy simulation of compressible turbulent channel flow with spectral difference method. AIAA P. **402** (2009). 47th AIAA Aerospace Sciences Meeting Including The New Horizons Forum and Aerospace Exposition, Orlando, FL, Jan 5–8, 2009, 15 p.

23. Liu, Y., Vinokur, M., Wang, Z.J.: Spectral difference method for unstructured grids I: basic formulation. Journal of Computational Physics **216**, 780–801 (2006)
24. Lodato, G., Castonguay, P., Jameson, A.: Discrete filter operators for large-eddy simulation using high-order spectral difference methods. Int. J. Numer. Meth. Fl. **72**(2), 231–258 (2013)
25. Lubcke, H., Schmidt, S., Rung, T., Thiele, F.: Comparison of LES and RANS in bluff-body flows. Journal of Wind Engineering and Industrial Aerodynamics **89**, 1471–1485 (2001)
26. Lyn, D., Einav, S., Rodi, W., Park, J.: A laser-Doppler velocimetry study of ensemble-averaged characteristics of the turbulent near wake of a square cylinder. J. Fluid Mech. **304**(1), 285–319 (1995)
27. Lyn, D., Rodi, W.: The flapping shear layer formed by flow separation from the forward corner of a square cylinder. J. Fluid Mech. **267**, 353–376 (1994)
28. Meister, A., Ortleb, S., Sonar, T.: On spectral filtering for discontinuous galerkin methods on unstructured triangular grids. Math. Schriften Kassel. (2009)
29. Nicoud, F., Ducros, F.: Subgrid-scale stress modelling based on the square of the velocity gradient tensor. Flow Turbul. Combust. **62**(3), 183–200 (1999)
30. Parsani, M., Ghorbaniasl, G., Lacor, C., Turkel, E.: An implicit high-order spectral difference approach for large eddy simulation. J Comp Phys **229**, 5373–5393 (2010)
31. Pasquetti, R.: High-order LES modeling of turbulent incompressible flow. C.R. Méc. **333**(1), 39–49 (2005)
32. Roe, P.L.: Approximate riemann solvers, parameter vectors and difference schemes. Journal of Computational Physics **43**, 357–372 (1981)
33. Taylor, M., Wingate, B.: The natural function space for triangular and tetrahedral spectral elements. Submitted to SIAM Journal on Numerical Analysis (1998)
34. Vincent, P.E., Castonguay, P., Jameson, A.: A new class of high-order energy stable flux reconstruction schemes. Journal of Scientific Computing **47**(1), 50–72 (2011)
35. Wang, B., Bergstrom, D.J.: A dynamic nonlinear subgrid-scale stress model. Physics of Fluids **17** (2005)
36. Winckelmans, G.S., Wray, A.A., Vasilyev, O.V., Jeanmart, H.: Explicit-filtering large-eddy simulation using the tensor-diffusivity model supplemented by a dynamic Smagorinsky term. Phys. Fluids **13**(5), 1385–1404 (2001)
37. Zang, Y., Street, R.L., Koseff, J.R.: A dynamic mixed subgrid-scale model and its application to turbulent recirculating flows. Phys. Fluids A-Fluid **5**(12), 3186–3196 (1993)